

Technical University of Denmark



## Offshore Code Comparison Collaboration within IEA Wind Task 23: Phase IV Results Regarding Floating Wind Turbine Modeling

**Jonkman, J.; Larsen, Torben J.; Hansen, Anders Melchior; Nygaard, T.; Maus, K.; Karimirad, M.; Gao, Z.; Moan, T.; Fylling, I.; Nichols, J.; Kohlmeier, M.; Pascual Vergara, J.; Merino, D.; Shi, W.**

*Published in:*

EWEC 2010 Proceedings online

*Publication date:*

2010

*Document Version*

Publisher's PDF, also known as Version of record

[Link back to DTU Orbit](#)

*Citation (APA):*

Jonkman, J., Larsen, T. J., Hansen, A. M., Nygaard, T., Maus, K., Karimirad, M., ... Shi, W. (2010). Offshore Code Comparison Collaboration within IEA Wind Task 23: Phase IV Results Regarding Floating Wind Turbine Modeling. In EWEC 2010 Proceedings online European Wind Energy Association (EWEA).

## DTU Library

Technical Information Center of Denmark

---

### General rights

Copyright and moral rights for the publications made accessible in the public portal are retained by the authors and/or other copyright owners and it is a condition of accessing publications that users recognise and abide by the legal requirements associated with these rights.

- Users may download and print one copy of any publication from the public portal for the purpose of private study or research.
- You may not further distribute the material or use it for any profit-making activity or commercial gain
- You may freely distribute the URL identifying the publication in the public portal

If you believe that this document breaches copyright please contact us providing details, and we will remove access to the work immediately and investigate your claim.

# A NOVEL FLOATING OFFSHORE WIND TURBINE CONCEPT: NEW DEVELOPMENTS

L. Vita, U.S.Paulsen, T.F.Pedersen  
Risø-DTU Technical University of Denmark, Roskilde, Denmark  
luca.vita@risoe.dk

## Abstract:

A novel concept for offshore floating wind turbines (Deep Wind) was presented by the authors in [1]. This paper deals with new developments of the novel concept. Three configurations, each with different degrees of freedom, have been selected to be presented in this paper. The first configuration, characterized by the lowest number of degrees of freedom, is investigated by an aero-elastic code.

**Keywords:** offshore, floating, vertical axis wind turbine, novel concept, aero-elastic code.

## 1 Introduction

The new European energy targets address an important role to wind energy. The installed wind power in Europe is expected to reach 230GW in 2020 (it was 120GW at the end of 2008). As reported in [2] 40GW are expected to come from off-shore wind power, meaning a growth of 28% in the annually new offshore power installation for the next 10 years. However offshore wind power is still more costly than onshore power (around the double of the cost [2]) and new solutions are needed in order to:

- Reduce the cost
- Exploit new offshore sites, such as deep seas.

The concept Deep Wind, here described, starts from the hypothesis that offshore wind energy needs new concepts specifically designed for offshore conditions. Starting from this hypothesis few issues are highlighted to be strategic for a successful offshore concept:

- Simplicity, in order to reduce the costs and facilitate the implementation of new solutions, for instance for O&M or for installation.
- Up-scaling potential.
- Suitability for deep sites.

Deep Wind is the synthesis of these three issues in a new floating offshore wind energy concept.

## 2 Deep Wind Concept

The whole concept, as presented in [1], is an innovative and simple way to look to offshore wind energy. It consists of a Darrieus rotor whose tower is extended underwater, in order to act as a spar buoy, as shown in Figure 1. The whole system is rotating and the power is generated by a generator placed at the bottom of the tower and fixed at the anchoring system.

The mean peculiarities of the concept are:

- A Darrieus rotor, whose tower is extended below the water surface, acting as a rotating spar buoy
- The generator is mounted at the bottom of the tower and acts as counter weight
- Control system is achieved by controlling the generator rotational speed
- Safety system with water brakes is suitable
- Specific O&M solutions are possible [1].

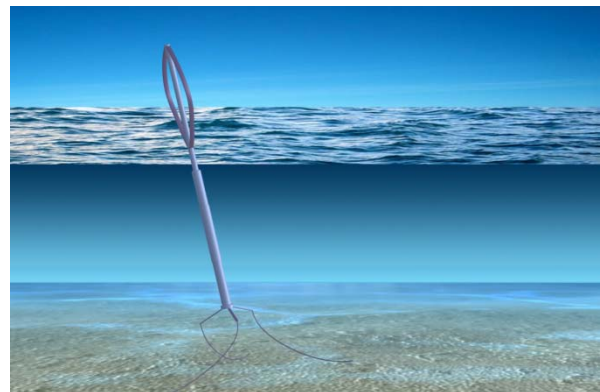


Figure 1 Artistic view of the concept

## 3 Description of the three configurations

Several configurations are possible for Deep Wind. Three of them have been selected to investigate the new concept.

### 3.1 First Configuration (Sea bed configuration)

The generator is fixed on the sea-bed and the shaft is extended to the sea bottom. The shaft has two rotational degrees of freedom: it can tilt back and forth and to the sides (pitch and roll).

This configuration has been selected to be investigated first, in order to verify that the concept works without serious vibrations and instabilities.

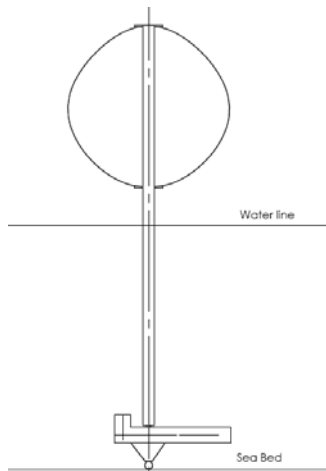


Figure 2 Schematic drawing of the first configuration (sea bed configuration)

### 3.2 Second Configuration (Torque arm fixed configuration)

The generator is mounted on a torque arm. Compared to the sea-bed configuration the shaft has one more translational degree of freedom, i.e. it can move up and down (heave).

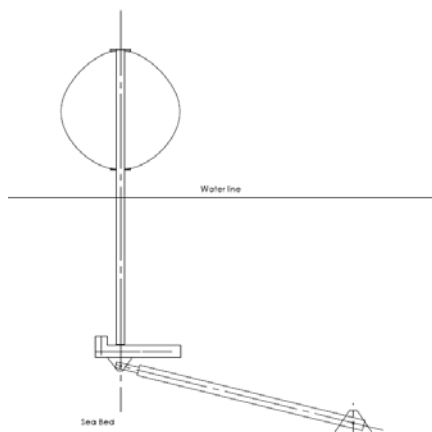


Figure 3 Schematic drawing of the second configuration (torque arm fixed configuration)

### 3.3 Third Configuration (Mooring fixed configuration)

Three torque arms are mounted to the generator box. The torque arms are connected to the sea bed by a mooring system. Compared to the previous configuration the shaft has two more translational degrees of freedom (sway and surge).

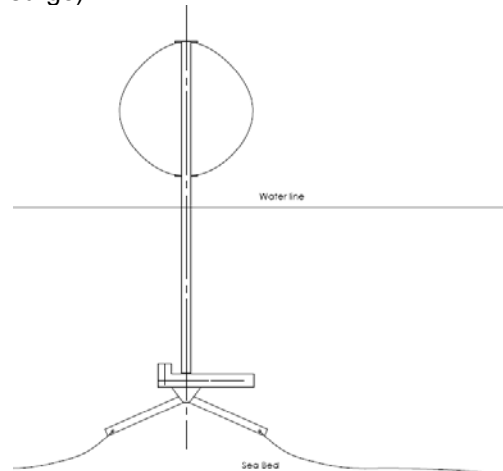


Figure 4 Schematic drawing of the third configuration (Mooring fixed configuration)

The degrees of freedom of the three configurations are summarized in the table below.

Table 1 Degrees of freedom of the three configurations

	Surge	Sway	Heave	Pitch	Roll
1 <sup>st</sup> Configuration				X	X
2 <sup>nd</sup> Configuration			X	X	X
3 <sup>rd</sup> Configuration	X	X	X	X	X

## 4 Methodology

The first configuration (Figure 2) has been selected to be investigated.

### 4.1 Loads

The loads acting on the structure have been classified in three kinds:

#### Gravitational loads:

The weight of the blades and the tower.

#### Aerodynamic loads

The torque, the thrust and side force on the rotor. The aerodynamic loads on the blades, not investigated in this paper.

### Hydrodynamic and hydrostatic loads

Buoyancy, Morrison's forces due to the waves interaction, friction moment due to the rotation in the water, lift and drag force due to the water currents passing on the rotating tube.

The loads generated by the external conditions are shown in a sketch in Figure 5, where:

Wsp: Wind speed

U: Water current speed

A, T: Significant wave height and wave period

T: Aerodynamic force on the rotor (thrust and side force)

Q: Aerodynamic torque

L: Hydrodynamic side force, perpendicular to the water current direction

Fm: Hydrodynamic forces in oscillatory flow (Morrison formulation)

Mf: Friction Moment

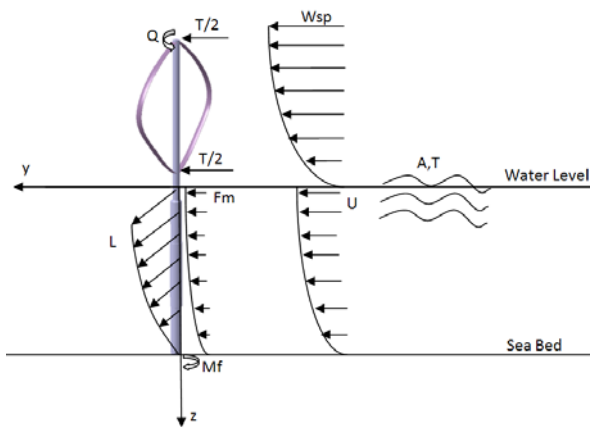


**Figure 5 External conditions and main loads on the turbine**

A first estimation of the loads on the structure is reported in Table 2.

**Table 2 Estimation of the magnitude of the loads on the turbine**

Loads	Estimated Magnitude *
Aerodynamic thrust	$2.4 \cdot 10^5$ N
Bending moment on the tower at the water surface	$1.1 \cdot 10^7$ Nm
Hydrodynamic lift (side force)	$2.16 \cdot 10^6$ N
Hydrodynamic friction	$2.2 \cdot 10^4$ Nm
Vertical Force at the bottom	$1.3 \cdot 10^7$ N

\* Values calculated at rated conditions, at wind speed 14m/s and with water currents of 1 m/s. Lift and friction are integrated on the whole submerged tower

## 4.2 Numerical code

For all numerical computations, the multi-body HAWC2 aero-elastic code is used [3]. The first version of HAWC2 was released in 2004 and the code has been implemented to investigate horizontal axis wind turbines (HAWT's). Recently it has also been used to simulate floating HAWT's [4]. As a multi-body formulation is used in HAWC2, the present floating VAWT design can be modeled without major changes in the code.

However some new features (such as a new aerodynamic formulation for VAWT and several dedicated dlls) are necessary, as shown in Figure 6.

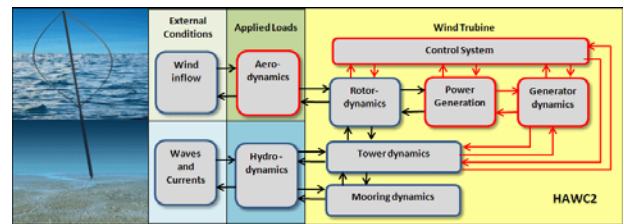


**Figure 6 Flow diagram of the HAWC2 code, in red the parts needing to be partially modified or added.**

At the present moment, the HAWC2 core is connected to the following dlls:

- Aerodynamic dll for VAWT, consisting of a double stream tube model. Correction for Reynolds number is included. Correction for the tilt angle of the rotor is not included.
- A slip generator model dll, simulating an induction generator. A starter dll is also included to start up the Darrieus rotor.
- A hydrodynamic dll, generating waves and current and calculating hydrodynamic forces using the Morrison equations.
- A dll, calculating the friction in the water and the lift and drag forces due to the current passing the rotating tower.

## 5 Study case

### 5.1 Dimensions and performance

A 2MW turbine has been selected in order to investigate the new concept. The main specifications of the system are reported in Table 3, versus the dimensions of a similar floating HAWC concept, Hy Wind.

**Table 3 Wind Deep dimensions for a 2MW size, compared to a floating horizontal axis wind turbine (Hy Wind)**

	Deep Wind	Hy Wind [5]
Power	2 MW	2.3 MW
Rotor Diameter	67 m	82.4 m
Rotor Height	75 m	65.0 m
Chord (blades number)	3.2 m (2)	(3)
Rotational speed at rated conditions	15.0 rpm	
Radius of the rotor tower	2.0 m	3.0 m
Maximum radius of the submerged part	3.5 m	4.15 m
Total tower length (underwater part)	183 m (93m)	165 (100)
Displacement	3000 tons	5300 tons

## 5.2 Load cases

Numerical simulations have been performed for three load cases. In each load case, the turbine is started up by a starter and the rotational speed is kept constant by the generator.

The wind speed shear generated in the code is not correlated with the computed water currents and waves.

### First load case

The reference wind speed is constant at 14m/s. A shear wind profile is used in the model with a roughness constant of  $z_0 = 0.0001$  (up to 10m/s) and 0.01 (for wind speeds above 10m/s). The reference wind speed is considered at the half of the rotor height, i.e. 52.5m. Turbulence effects are not considered. The wind direction is constantly on the y axis.

Regular waves are modeled. The direction of the waves is transversal to the direction of the wind (x axis). The significant wave height is 4.0m and the wave period is 9.0s, see Figure 7.

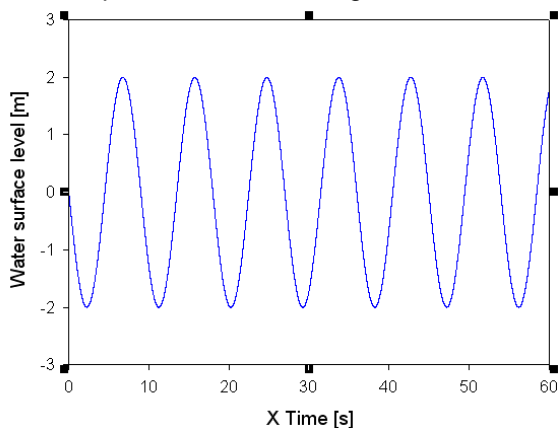


**Figure 7 z coordinate of the water surface plane**

### Second load case

In the second load case, the wind conditions are the same of the first load case.

The waves are not included in the model but water currents are added with direction constantly on the x axis.

The water current is constantly 1.0m/s at the water surface and zero at the sea bottom. The water shear profile (Figure 8) follows the equation:

$$U(z) = U_0 \left( \frac{z + wd}{wd} \right)^\alpha$$

Where:

z: water depth

U(z): water speed at z

$U_0$ : water speed at the water surface, i.e. 1m/s

wd: water depth

$\alpha$ : 0.5

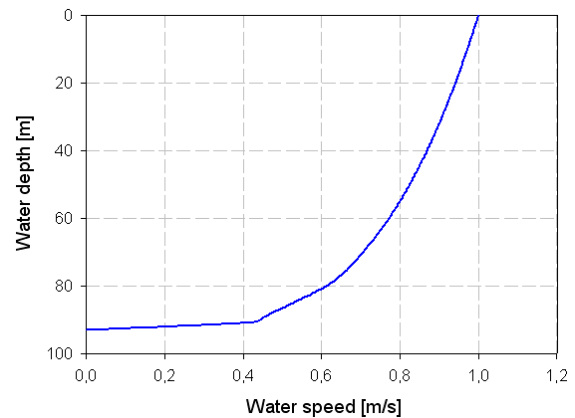


**Figure 8 Water shear profile**

### Third load case

In the third load case both waves and currents are added on the x directions.

The effect of the oscillatory flow on the water currents is visible in Figure 9. The wind speed profile remains the same.

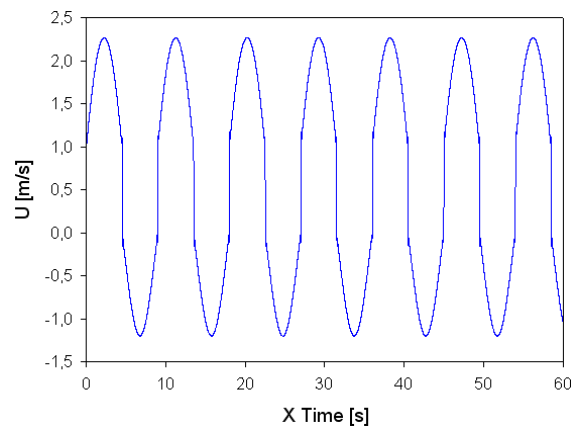


**Figure 9 Oscillatory flow at the water surface**

A summary of the load case is shown in Table 4.

**Table 4 Load cases summary**

	Wind	Waves	Currents
1 <sup>st</sup> load case	X		X
2 <sup>nd</sup> load case	X	X	
3 <sup>rd</sup> load case	X	X	X

## 6 Results

The three load cases are investigated in the time domain and in the frequency domain, by performing a power density spectrum analysis. In all the three cases the turbine is started by the generator, from a condition of  $\omega=0$  and  $\theta=0$ , with  $\omega$  and  $\theta$  respectively the rotational speed and the tilt angle of the turbine.

The most relevant natural frequencies of the system are summarized in Table 5.

**Table 5 Main frequencies of the system**

Mode	Frequency [Hz]
Turbine Pitching (around x)	0.27
Rolling (around y)	0.27
Yawing (around z)	1.07
1p (one blade rotation)	0.25
2p (two blades rotation)	0.50
Wave frequency	0.11

Below are reported the results of the computations for the three load cases. The results are reported in two sections: time domain and frequency domain. The parameters considered in the investigations are:

- Displacement dx and dy of the water surface cross section of the tower.
- Force Fx and Fy measured on the tower at the bottom of the blades (15m above the water surface level).
- Bending moment Mx and My measured at the water surface cross section of the tower.
- Vertical force Fz measure at the bottom of the tower.
- Hydrodynamic side force and friction moment, integrated on the first 20m of the tower below the sea surface plane.

### 6.1 Load case 1

#### Time domain

In the load case1 the waves are not computed. Therefore the water speed follows the shear profile of Figure 8 along the z coordinate. The water currents direction lays on the x axis and the

hydrodynamic side force acts on the y axis. In the Figure 10, the side force and the friction moment are shown. The absolute values of the force and the moment increase during the time, due to the dependence from the rotational speed. Once achieved the rated rotational speed, the moment and the force become constant (at t~120s).

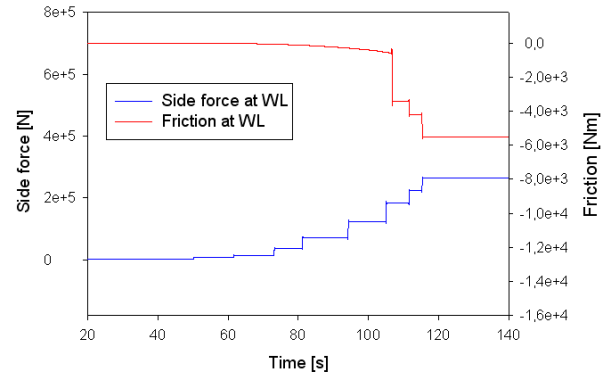


**Figure 10 Side force and friction moment integrated on the first 20m of the tower below the surface (Starting up two minutes time series)**

The other main loads on the structure are the aerodynamic forces on the rotor. In Figure 11, it is shown a time series of Fx, Fy. The time series is divided in two sections: starting conditions (30s-60s) and rated conditions (300s-350s). As neither waves nor rotational speed are present, the forces are equal to zero at the starting of the turbine. At the rated conditions the forces are reflecting the behavior of the aerodynamic force: a side force Fx, harmonic with a null average value; a thrust force Fy with a not null average value.

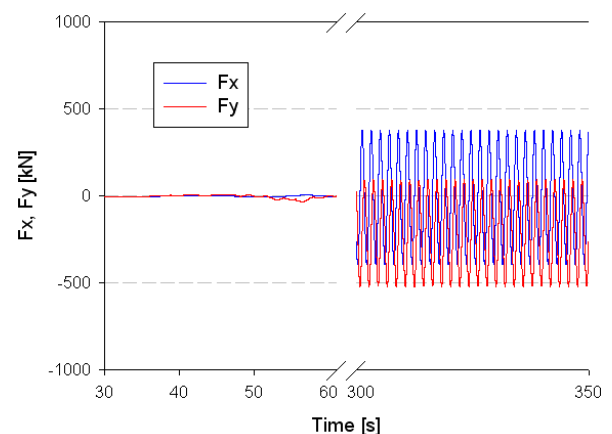


**Figure 11 Fx, Fy on the tower section 15m above the sea. First time series (30-60s) with no rotation of the rotor, second time series (300-350s) at rated conditions**

The resulting trajectory at these conditions is shown in a polar graph in Figure 12. The turbine reaches the equilibrium at  $Y_0=26.5\text{m}$  and  $X_0=1\text{m}$ , corresponding to a tilt angle of 16.5 degrees.

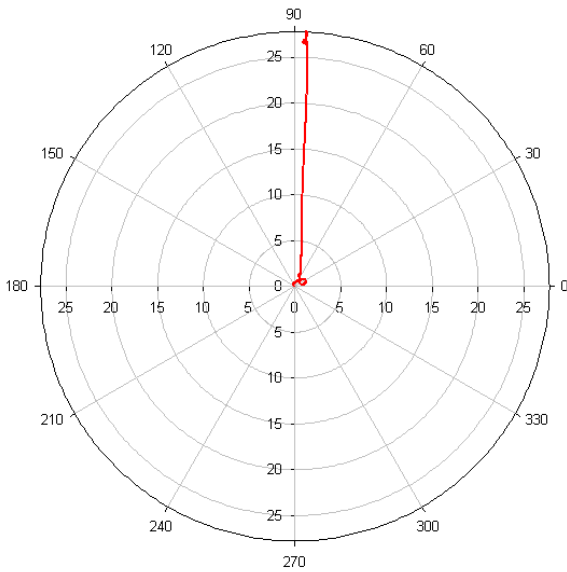


**Figure 12 Trajectory of the surface section of the tower in the water surface plane xy**

**Frequency domain**

The influence of the aerodynamic forces on the displacements is evident also in the frequency domain. In Figure 13,  $dy$  reach the peak at the 2p frequency (0.5Hz). The same it is visible in Figure 14 for the DSP of  $F_z$ .

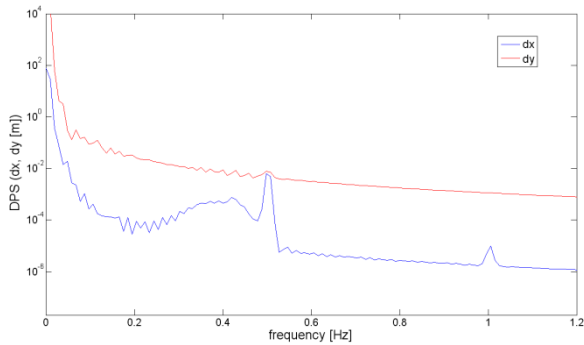


**Figure 13 Density power spectrum of the displacement dx, dy**

The two components of the bending moment reach the peak at the odd rotor frequencies (1p and 3p), see Figure 15.

Finally in Figure 16, it is shown the DSP of the component  $F_x$  and  $F_y$ . The 2p frequency and the higher harmonic are visible.

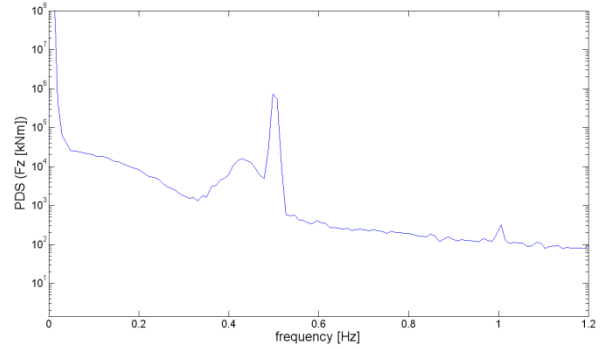


**Figure 14 Density power spectrum of  $F_z$**

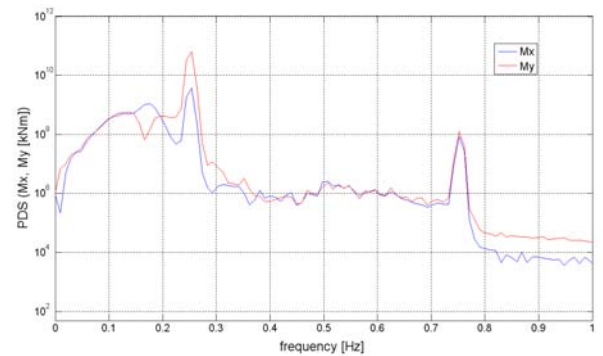


**Figure 15 Density power spectrum of the bending moments  $M_x, M_y$ , at the water surface plane**

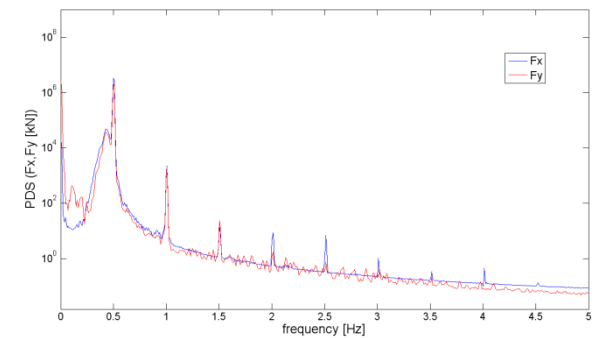


**Figure 16 Density power spectrum of the force on the rotor,  $F_x, F_y$**

**6.2 Load case 2**

**Time domain**

The presence of waves in the system introduces a force  $F_x$  on the rotor even if the system is not rotating yet, see Figure 17 (first 60s). Also the plot of  $F_x$  and  $F_y$  at rated condition (Figure 17, 300s-350s) is quite different from the load case1 (Figure 11).

The trajectory of the tower is traced in Figure 18. At the equilibrium  $Y_0=-0.75\text{m}$  and  $X_0=-0.25$ , corresponding to a tilt angle lower than 1 degree. The system describes an elliptical motion around this point, where the axis of the ellipsis

correspond to the amplitude of the oscillations around  $X_0$  and  $Y_0$ , i.e.  $dx=2.10\text{m}$  and  $dy=0.50\text{m}$ .

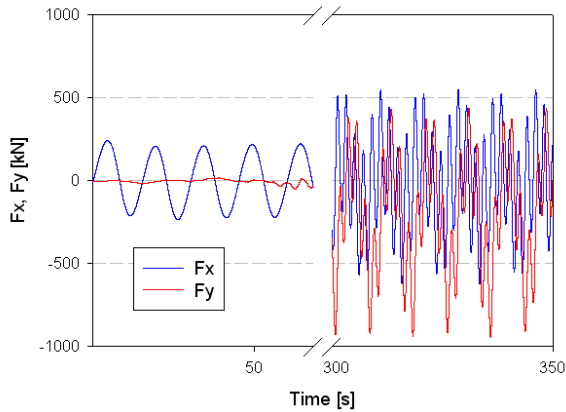


**Figure 17**  $F_x$ ,  $F_y$  on the tower section 15m above the sea. First time series (20-60s) with no rotation of the rotor, second time series (300-350s) at rated conditions

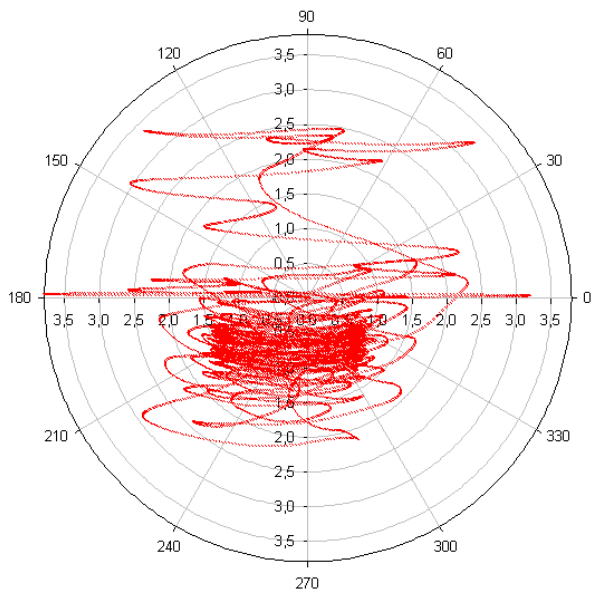


**Figure 18** Trajectory of the surface section of the tower in the water surface plane  $xy$

**Frequency domain**

The waves effect on the displacements of the turbine is also visible from the Figure 19, where a peak at the wave frequency (0.11Hz) is achieved. The same peak is achieved for the forces  $F_z$  (Figure 22), the hydrodynamic side force (Figure 21) and  $F_x$  (Figure 20). However the  $F_y$  is still shown a stronger dependency by the rotational frequencies, see Figure 20.

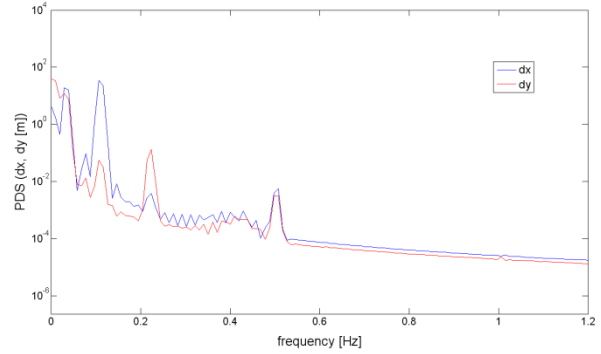


**Figure 19** Density power spectrum of the displacement  $dx$ ,  $dy$

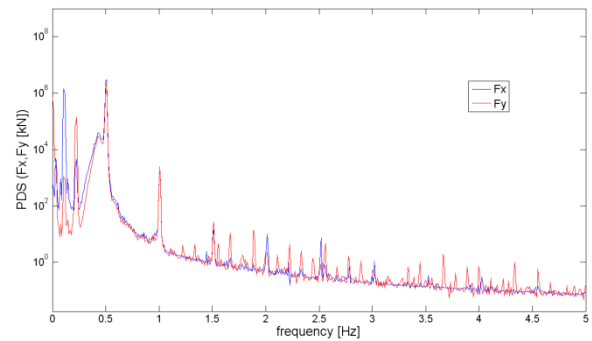


**Figure 20** Density power spectrum of the force on the rotor,  $F_x$ ,  $F_y$

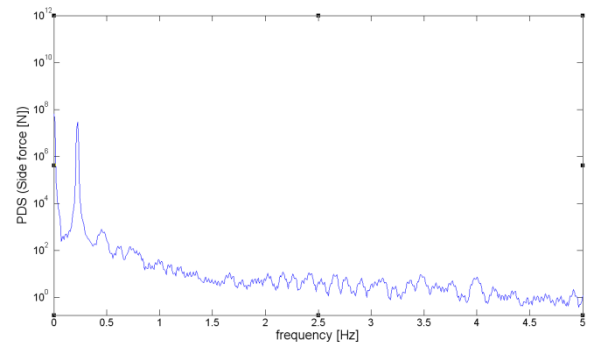


**Figure 21** Density power spectrum of the hydrodynamic side force

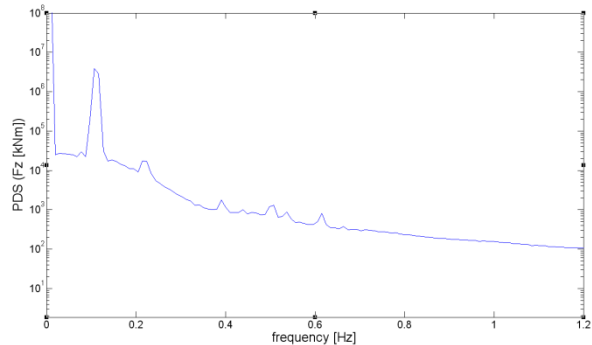


**Figure 22** Density power spectrum of the vertical force  $F_z$

### 6.3 Load case 3

#### Time domain

As both waves and currents are computed, the hydrodynamic forces and friction oscillate with high amplitude, see Figure 23. Time series of  $F_x$  and  $F_y$  are reported in Figure 24, the chart it is very similar to the load case2 (Figure 17).

The trajectory described by the tower is shown in Figure 25. The equilibrium is achieved at  $X_0=1.25m$  and  $Y_0=27.1$ , corresponding to a tilt angle of 17 degrees. As in the second load case, at the equilibrium the turbine describes an elliptic motion around  $(X_0, Y_0)$ , see Figure 26. The amplitude of this motion is  $dx=2m$  and  $dy=3.8m$ .

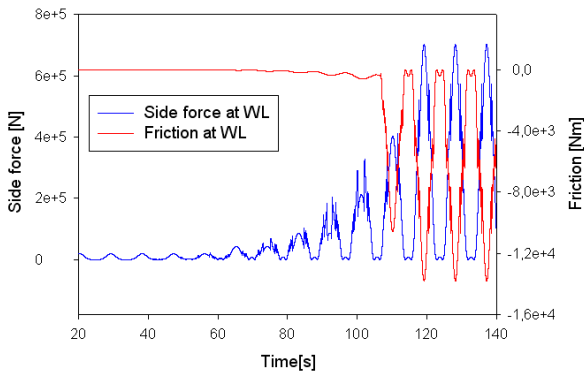


Figure 23 Side force and friction moment, integrated on the first 20m of the tower below the surface (Starting up two minutes time series)

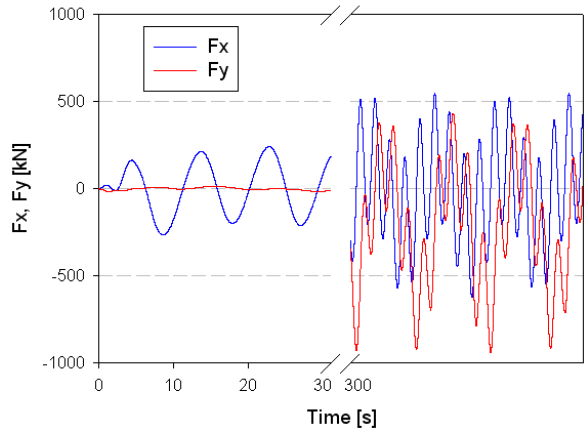


Figure 24  $F_x$ ,  $F_y$  on the tower section 15m above the sea. First time series with no rotation of the rotor, second time series at rated conditions

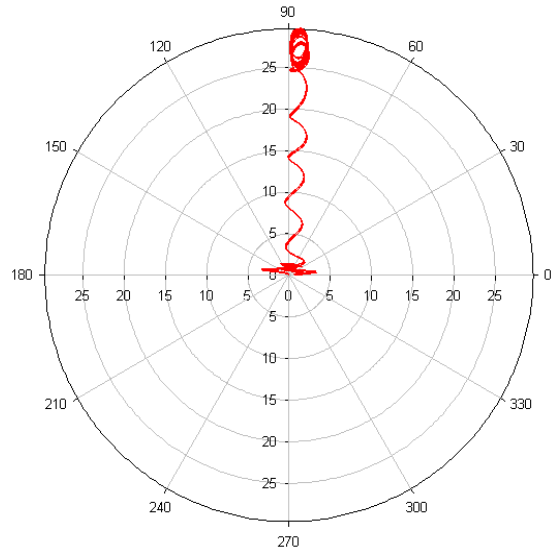


Figure 25 Trajectory of the surface section of the tower in the water surface plane xy

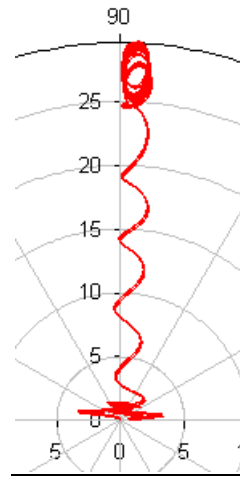


Figure 26 Zoom in of Figure 25, the ellipsis described by the turbine trajectory is visible

#### Frequency domain

As the currents are included in the computation of this load case, the wave frequency becomes dominant also in the displacement along the  $y$  direction, see Figure 27.

In the meantime, due to the large displacements, the dominant frequency of  $F_z$  (Figure 28) is  $2p$  as in the first load case (Figure 14).

Both the rotational and the waves frequencies are noticeable for the  $F_x$  and  $F_y$ , in Figure 29.

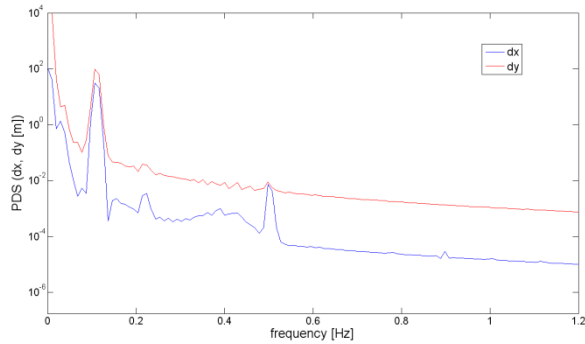


**Figure 27 Density power spectrum of the displacements dx, dy**

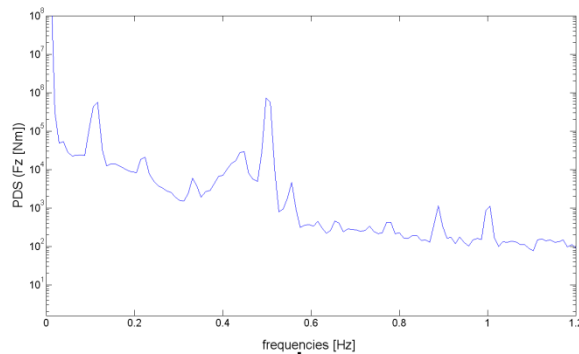


**Figure 28 Density power spectrum of the vertical force on the rotor, Fz**

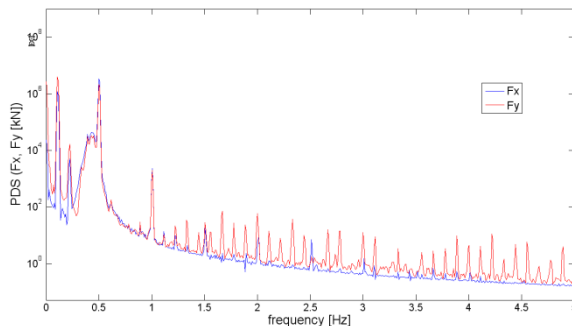


**Figure 29 Density power spectrum of the force on the rotor, Fx, Fy**

## 7 Discussion

The results show a strong coupling between the pitch and the roll motions of the system. This is partially due to the fact that the turbine acts as a gyro during its motion. This means that when the tower is turning, every load on the x direction causes a reaction also on the y direction.

Another reason for the coupling of the two motions is the nature of the hydrodynamic side force, generating a load on the direction transversal to the current direction. Thus a variation of the waves intensity on the x direction, it will effect also the equilibrium along the y

direction, as for instance comparing Figure 13 and Figure 27.

Another strong coupling exists between aerodynamic and hydrodynamic loads. Indeed the hydrodynamic forces and the friction moment are strongly dependent by the rotational speed of the rotor, see Figure 23. Therefore the optimization of the aerodynamic design of the rotor has to include an optimization of the hydrodynamic loads on the structure.

However the hydrodynamic loads seem to be dominant in the dynamics of the system, as anticipated in Table 2. Indeed the turbine operates with a tilt angle, strongly dependent by the water currents speed. Once the turbine achieves the equilibrium, the tower experiences an elliptical motion on the water surface plane. The amplitude of the elliptical motion seems to be strongly dependent by the amplitude of the waves, as comparing Figure 12 and Figure 25.

## 8 Conclusions

A new concept for floating offshore vertical axis wind turbine has been presented and a method to investigate the concept has been proposed, based on the number of degrees of freedom. A particular configuration for the concept has been selected and investigated using an aero-elastic code.

The computations have been carried out for three load cases, changing the wind and hydrodynamic external conditions. The changing of the external conditions is reflected in different values of the tilt angle of the wind turbine at nominal power conditions.

Further investigations are still needed, especially in order to investigate:

- the influence of the tilt angle on the aerodynamic computations
- the interaction between the water close to the surface and the tower, during its elliptic motion

However experimental results in an ocean basin would be still needed to fully validate the numerical results.

## References

1. "A Novel floating offshore wind turbine concept", Vita L, Paulsen US, Pedersen TF, Madsen HA, Rasmussen F - EWEC 2009

2. *"Oceans of Opportunity", Fichaux N, Wilkes J - EWEA 2009"*
3. *"How HAWC2, The user's manual", T.J. Larsen and A.M. Hansen. Risø-R-1597, 2008*
4. *"Integrated Dynamic Analysis of Floating Offshore Wind Turbines", Skaare B and al.*
5. *"HYWIND, Concept, challenges and opportunities ", Statoil*